

# Composition and wavelength dependence of the refractive index in $\text{Cd}_{1-x}\text{Mn}_x\text{Te}$ epitaxial layers

D. W. Schubert, M. M. Kraus, R. Kenklies, C. R. Becker,  
and R. N. Bicknell-Tassius  
Physikalisches Institut der Universität Würzburg, D-8700 Würzburg, Germany

(Received 9 September 1991; accepted for publication 25 February 1992)

We have investigated  $\text{Cd}_{1-x}\text{Mn}_x\text{Te}$  thin films with Mn concentrations of  $x=0.12, 0.18, 0.30, 0.52,$  and  $0.70$ . These single crystal layers were grown by molecular beam epitaxy on  $[001]$  CdTe substrates. The real part of the refractive index,  $n$ , was determined below the band-gap  $E_0$  in the range of  $0.5\text{--}2.5$  eV at  $T=300$  K. The parallel reflectivity was measured near the Brewster angle at the YAG laser wavelength of  $1.064 \mu\text{m}$  ( $h\nu=1.165$  eV). Combining these results with the optical pathlength results ( $\tilde{n}d$ ) of reflection measurements in a Fourier spectrometer we have determined  $n(x,\nu)$  over a wide spectral range by utilizing a three parameter fit. The accuracy of these results for  $n$  should improve waveguide designs based on this material.

The ternary II-VI semiconductor  $\text{Cd}_{1-x}\text{Mn}_x\text{Te}$  (CdMn)Te is a typical representative of the group of dilute magnetic semiconductors (DMS). The magnetic moments of the  $\text{Mn}^{2+}$  ions in (CdMn)Te arise from their  $3d^5$  electrons. This material behaves much the same as ordinary semiconductors in the absence of a magnetic field. Depending on the Mn concentration  $0 < x < 0.7$  the energy gap varies from  $1.52$  to  $2.44$  eV at  $T=295$  K.<sup>1</sup> (CdMn)Te exhibits many new and interesting properties when a magnetic field is applied. These include extremely large magneto-optical effects, i.e., large Faraday rotation and giant Stokes shift in spin-flip Raman scattering.<sup>2</sup> During the past years, additional interest in this material has been stimulated by the improved growth of thin films by molecular beam epitaxy on various substrates such as GaAs<sup>3</sup> and CdTe.<sup>4</sup> To date, most of the optical studies have concentrated on MBE grown single layers,<sup>5</sup> multiple quantum wells and superlattices.<sup>6-8</sup>

Accurate values for the refractive index  $n$  are important for waveguide related applications of (CdMn)Te

films. The refractive index of bulk CdTe was investigated very early by Marple in a prism refraction experiment.<sup>9</sup> The first investigations of (CdMn)Te thin films on glass substrates were carried out by evaluation of transmission spectra by Miotkowski *et al.*<sup>10</sup> In this letter we have investigated the composition and wavelength dependence of the refractive index of (CdMn)Te films by combining two different reflection experiments.

The (CdMn)Te were grown on CdTe  $[100]$  substrates by MBE in a Riber 2300 system. Details of this system and the growth technique of this material have been previously published.<sup>4</sup> The Mn concentration of the samples was determined by photoluminescence measurements, which showed good homogeneity.

In our first reflection experiment we determined the refractive index  $n$  from the angular dependent parallel reflectivity near the Brewster angle at the YAG laser wavelength of  $\lambda=1.064 \mu\text{m}$ . Because of the two interfaces, air/(CdMn)Te and (CdMn)Te/CdTe substrate, we observed angular dependent interference. The back of the substrate has a rough surface so reflection from that side was negligible. At several locations on the sample we measured dif-

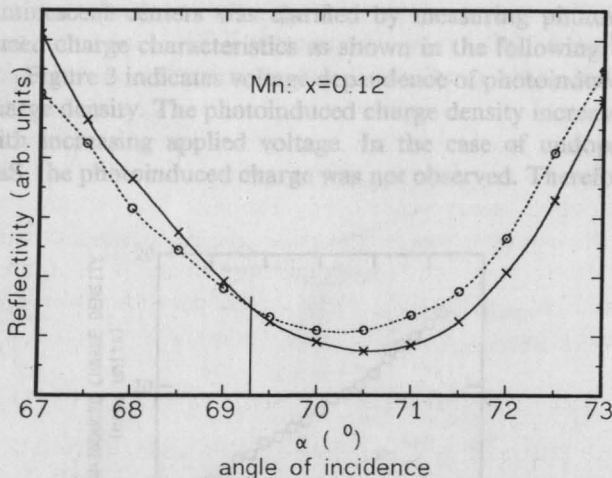


FIG. 1. Angular dependent parallel reflectivity with interferences of a  $\text{Cd}_{1-x}\text{Mn}_x\text{Te}$  film near the Brewster angle at  $\lambda=1.064 \mu\text{m}$  and  $T=300$  K. Crosses and solid line show measured reflectivity and a numerical fit using cyclic splines. Circles and dashed line show measured reflectivity and a numerical fit using cyclic splines. Solid and dashed curves represent reflectivities at different locations on the film.

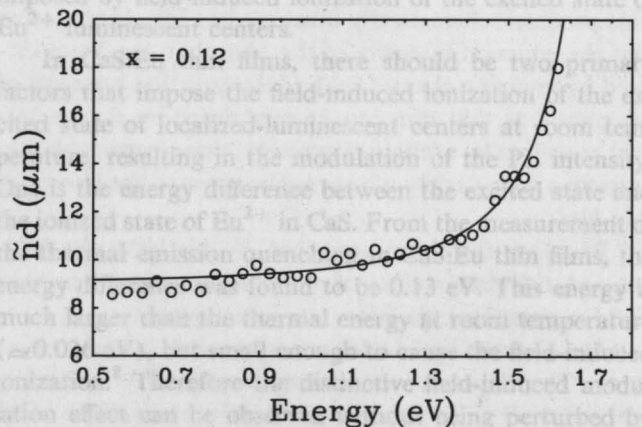


FIG. 2. Spectral dependence of the optical pathlength  $\tilde{n}d$  for a  $\text{Cd}_{1-x}\text{Mn}_x\text{Te}$  ( $x=0.12$ ) film. The circles represent the results of interferometric reflection measurements in a Fourier Spectrometer at  $T=300$  K. The solid line is a numerical fit utilizing the dispersion relationship given in the text, Eq. (2).

TABLE I. Directly measured refractive index  $n$  at  $\lambda=1.064 \mu\text{m}$  for five different  $\text{Cd}_{1-x}\text{Mn}_x\text{Te}$  films with Mn concentration  $x$ , average film thickness  $d$  and the dispersion formula parameters  $A$ ,  $B$ , and  $C$  as mentioned in the text.

Mn: $x$	$n$	$d$ ( $\mu\text{m}$ )	$A$	$B$ ( $\text{eV}^{-2}$ )	$C$ (eV)
$0.12 \pm 0.01$	$2.63 \pm 0.04$	3.50	6.75	0.12	1.835
$0.18 \pm 0.01$	$2.60 \pm 0.04$	1.74	6.50	0.12	1.918
$0.30 \pm 0.03$	$2.49 \pm 0.06$	1.21	6.22	0.12	2.112
$0.52 \pm 0.03$	$2.48 \pm 0.04$	1.65	5.95	0.12	2.622
$0.70 \pm 0.04$	$2.48 \pm 0.04$	1.13	5.81	0.12	3.210

ferent reflectivities for the same angle of incidence as a result of film thickness variation. Figure 1 shows typical reflectivity of the layer near the Brewster angle. Analysis of the common intersection allows an accurate determination of the refractive index.

In our second reflection experiment we determined the spectral dependence of the refractive index. The reflection from the samples was measured in the range from 0.5 to 2.5 eV with a commercial Bruker IFS 88 Fourier transform spectrometer. A tungsten lamp was used as a light source and a standard deuteriated triglycine sulfide detector. To improve the signal to noise ratio for photon energies higher than 1.1 eV, a Si detector was employed. Because the thickness of the epitaxial layers is on the order of several micrometers, pronounced interference fringes were observed. Neglecting second order terms one obtains the following relationship from the condition of constructive or destructive interference

$$\frac{1}{2d\Delta\nu} \cong n + \nu \frac{dn}{d\nu} = \tilde{n} \quad (1)$$

where  $n$ ,  $d$ ,  $\Delta\nu$  are the refractive index, film thickness, and the spectral separation in wavenumbers of two adjacent maxima or minima in the reflection spectrum, respectively. It should be pointed out, that only the product  $\tilde{n}d$  is assessable in this experiment. In Fig. 2 a typical spectral dependence of the optical pathlength  $\tilde{n}d$  is shown. For the purpose of this investigation the determination of the film thickness from the growth parameters alone is not accurate

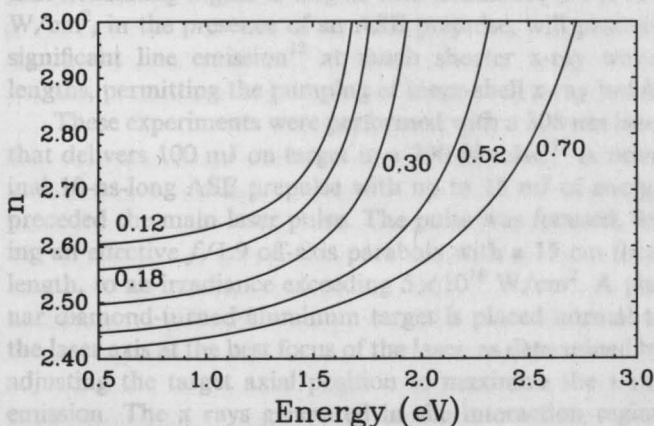


FIG. 3. The spectral dependence of the refractive index for different Mn concentrations ( $x=0.12, 0.18, 0.3, 0.52$ , and  $0.7$ ) of  $\text{Cd}_{1-x}\text{Mn}_x\text{Te}$  films, as given by Eq. (2).

enough. However, the index of refraction at one particular photon energy has been determined by the first method described above. To obtain an analytic expression for  $n(x, \nu)$  we have used the three parameter dispersion relationship,

$$n^2 = A + \frac{BE^2}{1 - (E/C)^2} \quad E < C. \quad (2)$$

Due to the secondary condition that the parameters  $A$ ,  $B$ , and  $C$  must be consistent with the measured refractive index at the YAG wavelength,  $n(x, \nu)$  can be determined using Eqs. (1) and (2).

The values obtained for the samples investigated are listed in Table I. For Mn concentrations from  $x=0$  to  $x=0.70$  the following relationships for the parameters  $A$ ,  $B$ , and  $C$  were deduced.

$$A(x) = 7.40 - 6.652x + 10.851x^2 - 6.553x^3, \quad (3)$$

$$B(x) = 0.12 \text{ (eV)}^{-2}, \quad (4)$$

$$C(x) = 1.655 + 1.411x - 0.118x^2 + 1.824x^3 \text{ eV}. \quad (5)$$

The calculated dispersion curves for our investigated films are plotted in Fig. 3. It can be seen that the refractive index decreases with increasing Mn concentration as expected for the normal dispersion of a direct gap semiconductor.<sup>11</sup>

In conclusion we have determined the refractive index for  $(\text{CdMn})\text{Te}$  films over a wide spectral range with good accuracy. Improved  $p$ - and  $n$ -type doping, lateral structuring, and metallic contacting techniques would favor this large band-gap material for integrated and electro-optical devices such as laser diodes, modulators, or optical switches in a waveguide configuration.

This project was supported by the Bundesministerium für Forschung und Technologie in Bonn. The authors would like to thank A. Waag for his contribution to epitaxial growth.

<sup>1</sup>R. Bücker, H.-E. Gumlich, and M. Krause, J. Phys. C: Solid State Phys. **18**, 661 (1985).

<sup>2</sup>N. B. Brandt and V. V. Moshchalkov, Adv. Phys. **33**, 193 (1984).

<sup>3</sup>L. A. Kolodziejski, T. C. Bonsett, R. L. Gunshor, S. Datta, R. B. Bylisma, M. W. Becker, and N. Otsuka, Appl. Phys. Lett. **45**, 440 (1984).

<sup>4</sup>R. N. Bicknell-Tassius, A. Waag, Y. S. Wu, T. A. Kuhn, and W. Ossau, J. Cryst. Growth **101**, 31 (1990).

<sup>5</sup>W. Limmer, S. Bauer, H. Leiderer, W. Gebhardt, and R. N. Bicknell-Tassius, J. Phys.: Condens. Matter **2**, 8669 (1990).

<sup>6</sup>R. N. Bicknell-Tassius, R. W. Yanka, N. C. Giles-Taylor, D. K. Blanks, E. L. Buckland, and J. F. Schetzina, *Appl. Phys. Lett.* **45**, 92 (1984).  
<sup>7</sup>D. K. Blanks, R. N. Bicknell-Tassius, N. C. Giles-Taylor, J. F. Schetzina, A. Petrou, and J. Warnock, *J. Vac. Sci. Technol. A* **4**, 2120 (1986).  
<sup>8</sup>R. L. Harper, Jr., R. N. Bicknell-Tassius, D. K. Blanks, N. C. Giles, J.

F. Schetzina, Y. R. Lee, and A. K. Ramdas, *J. Appl. Phys.* **65**, 624 (1989).  
<sup>9</sup>D. T. F. Marple, *J. Appl. Phys.* **35**, 539 (1964).  
<sup>10</sup>I. Miotkowski and S. Miotkowska, *Thin Solid Films* **165**, 91 (1988).  
<sup>11</sup>S. H. Wemple and M. Di Domenico, Jr., *Phys. Rev. B* **3**, 1338 (1971).

Energy (eV)	0.12	0.18	0.30	0.50	0.70	1.00
0.17 ± 0.01	0.17 ± 0.01	0.17 ± 0.01	0.17 ± 0.01	0.17 ± 0.01	0.17 ± 0.01	0.17 ± 0.01
0.18 ± 0.01	0.18 ± 0.01	0.18 ± 0.01	0.18 ± 0.01	0.18 ± 0.01	0.18 ± 0.01	0.18 ± 0.01
0.20 ± 0.03	0.20 ± 0.03	0.20 ± 0.03	0.20 ± 0.03	0.20 ± 0.03	0.20 ± 0.03	0.20 ± 0.03
0.22 ± 0.03	0.22 ± 0.03	0.22 ± 0.03	0.22 ± 0.03	0.22 ± 0.03	0.22 ± 0.03	0.22 ± 0.03
0.26 ± 0.04	0.26 ± 0.04	0.26 ± 0.04	0.26 ± 0.04	0.26 ± 0.04	0.26 ± 0.04	0.26 ± 0.04

These single crystal layers were grown by molecular beam epitaxy on (100) GaAs. The growth rate was determined by the thickness of the layers. The refractive index of the layers was determined by the reflectivity of the layers. The common interface energy of the layers was determined by the reflectivity of the layers. The common interface energy of the layers was determined by the reflectivity of the layers.

In our second reflection experiment we determined the spectral dependence of the refractive index. The reflection from the samples was measured in the range from 0.2 to 2.5 eV with a commercial photodiode array detector. A tungsten lamp was used as a light source and a standard beam splitter was used to split the light. The signal to noise ratio for photon counting was improved by using a lock-in amplifier. The lock-in amplifier was set to a frequency of 1.15 kHz. The lock-in amplifier was set to a frequency of 1.15 kHz.

The common interface energy of the layers was determined by the reflectivity of the layers. The common interface energy of the layers was determined by the reflectivity of the layers. The common interface energy of the layers was determined by the reflectivity of the layers. The common interface energy of the layers was determined by the reflectivity of the layers.

In our first reflection experiment we determined the spectral dependence of the refractive index. The reflection from the samples was measured in the range from 0.2 to 2.5 eV with a commercial photodiode array detector. A tungsten lamp was used as a light source and a standard beam splitter was used to split the light. The signal to noise ratio for photon counting was improved by using a lock-in amplifier. The lock-in amplifier was set to a frequency of 1.15 kHz. The lock-in amplifier was set to a frequency of 1.15 kHz.

The common interface energy of the layers was determined by the reflectivity of the layers. The common interface energy of the layers was determined by the reflectivity of the layers. The common interface energy of the layers was determined by the reflectivity of the layers. The common interface energy of the layers was determined by the reflectivity of the layers.

The common interface energy of the layers was determined by the reflectivity of the layers. The common interface energy of the layers was determined by the reflectivity of the layers. The common interface energy of the layers was determined by the reflectivity of the layers. The common interface energy of the layers was determined by the reflectivity of the layers.

